BIOCHEMICAL PHARMACOLOGY 75 (2008) 527–537

available at www.sciencedirect.com

ScienceDirect

journal homepage: www.elsevier.com/locate/biochempharm

Efficient oxidation of promutagenic hydroxymethylpyrenes by cDNA-expressed human alcohol dehydrogenase ADH2 and its inhibition by various agents

Ronny Kollock [a], *Walter Meinl* [a], *Heiko Schneider* [a], *Monika Batke* [a], *Heinz Frank* [b], *Albrecht Seidel* [b], *Hansruedi Glatt* [a,*]

[a] *German Institute of Human Nutrition Potsdam-Rehbruecke, Department of Nutritional Toxicology, 14558 Nuthetal, Germany*
[b] *Biochemical Institute for Environmental Carcinogens, Prof. Dr. Gernot Grimmer Foundation, 22927 Grosshansdorf, Germany*

ARTICLE INFO

Article history:
Received 11 July 2007
Accepted 28 August 2007

Keywords:
ADH2
Alkylated polycyclic aromatic hydrocarbons
Benzylic alcohols
Detoxification
Sulphotransferase

ABSTRACT

Alkylated polycyclic aromatic hydrocarbons can be metabolically activated via benzylic hydroxylation and sulphation to electrophilically reactive esters. However, we previously found that the predominant biotransformation route for the hepatocarcinogen 1-hydroxymethylpyrene (1-HMP) in the rat *in vivo* is the oxidation of the side chain by alcohol dehydrogenases (ADHs) and aldehyde dehydrogenases to the carboxylic acid. Inhibition of this pathway by ethanol (competing ADH substrate) or 4-methylpyrazole (ADH inhibitor) led to a dramatic increase in the 1-HMP-induced DNA adduct formation in rat tissues in the preceding study. In order to elucidate the role of individual ADHs in the metabolism of alkylated polycyclic aromatic hydrocarbons, we expressed the various members of the human ADH family in bacteria. Cytosolic preparations from bacteria expressing ADH2 clearly oxidized hydroxymethylpyrene isomers (1-, 2- and 4-HMP) with the highest rate. This form was purified to near homogeneity to perform detailed kinetic analyses. High catalytic efficiencies (V_{max}/K_m) were observed with HMPs. Thus, this value was 10,000-fold higher for 2-HMP than for the reference substrate, ethanol. The corresponding aldehydes were also efficiently reduced by ADH2. 4-Methylpyrazole inhibited the oxidation of the HMP isomers as well as the reverse reaction. Daidzein, cimetidine and the competing substrate ethanol were further compounds that inhibited the ADH2-mediated oxidative detoxification of 1-HMP.

1. Introduction

Polycyclic aromatic hydrocarbons (PAHs) are important environmental carcinogens, present *e.g.* in cigarette smoke, diesel exhaust and foods [1]. Numerous congeners contain alkyl substituents or alkano bridges (alk-PAHs). PAHs require metabolic activation to reactive intermediates in order to become carcinogenic. Epoxidation, in particular the formation of vicinal dihydrodiol-epoxides, is a major mechanism for the activation of purely aromatic PAHs [1,2]. This mechanism may

* Corresponding author. Tel.: +49 33200 88321; fax: +49 33200 88426.
E-mail address: glatt@dife.de (H. Glatt).

Abbreviations: ADH, alcohol dehydrogenase; ALDH, aldehyde dehydrogenase; alk-PAH, alkylated polycyclic aromatic hydrocarbon; BSA, bovine serum albumin; CYP, cytochrome P450; DMSO, dimethylsulphoxide; FP, formylpyrene; FPLC, fast-performance liquid chromatography; HMP, hydroxymethylpyrene; mp, melting point; PAGE, polyacrylamide gel electrophoresis; PAH, polycyclic aromatic hydrocarbon; PCR, polymerase chain reaction; RT, reverse transcription; SDS, sodium dodecyl sulphate; SULT, sulphotransferase.

0006-2952/$ – see front matter
doi:10.1016/j.bcp.2007.08.030

also occur with some alk-PAHs. However, the side chain allows additional activation mechanisms, in particular the hydroxylation in the benzylic position by cytochromes P450 (CYPs) and subsequent formation of reactive sulphuric acid esters by sulphotransferases (SULTs) [3–5].

1-Methylpyrene is a substance that perfectly fits in this model. Although it does not contain a terminal benzo ring and thus cannot be activated to a vicinal dihydrodiol-epoxide, it is hepatocarcinogenic in newborn mice [6]. The parent PAH, pyrene, is considered to be non-carcinogenic. Thus the side chain is important for the carcinogenic activity. We have demonstrated that 1-hydroxymethylpyrene (1-HMP) is a major metabolite of 1-methylpyrene in rat and human hepatic microsomal systems as well as in V79-derived cell lines expressing various individual rat and human CYPs [7]. 1-HMP is strongly mutagenic to *Salmonella typhimurium* TA98 when incubated in the presence of rat and human hepatic cytosolic fraction supplemented with 3′-phoshoadenosine-5′-phosphosulphate, the cofactor for SULTs [8,9]. Likewise, a large number of cDNA-expressed rat and human SULTs are able to catalyze the activation of 1-HMP to a mutagen [10,11].

However, the predominant metabolic pathway of 1-HMP in the rat *in vivo* is its oxidation by alcohol dehydrogenases (ADHs) and subsequently aldehyde dehydrogenases (ALDHs) to its carboxylic acid [12]. Moreover, concurrent administration of ethanol (a competing substrate of ADH) or 4-methylpyrazole (a competitive inhibitor of ADH [13,14]) inhibited this pathway and led to a dramatic (up to 200-fold) increase in the level of DNA adducts formed in rats treated with 1-HMP [12]. A scheme of these pathways is presented in Fig. 1.

In order to elucidate the role of individual ADHs in the metabolism of alk-PAHs and to specify interactions with other compounds, such as ethanol, we expressed the various members of the human ADH family [15] in bacteria. Using cytosolic preparations we demonstrate that ADH2 is the form that most efficiently oxidizes the HMP isomers (1-, 2- and 4-HMP). This enzyme was then purified to near homogeneity to conduct kinetic analyses and interaction studies.

2. Materials and methods

2.1. Commercial chemicals, oligonucleotides and enzymes

4-Methylpyrazole, daidzein, cimetidine, 1-formylpyrene (1-FP), NAD^+ and NADH were purchased from Sigma–Aldrich (Taufkirchen, Germany). Oligonucleotides were purchased from BioTez (Berlin, Germany). Restriction endonucleases were obtained from Fermentas (St. Leon-Rot, Germany) and NEB (Frankfurt/M., Germany).

2.2. Syntheses

UV spectra were recorded on a Shimadzu UV-1601 spectrophotometer. NMR spectra were obtained on Bruker AMX400 and DRX500 spectrometers in either $CDCl_3$ or DMSO-d_6. Melting points (mp) were determined on a Büchi 510 apparatus. Silica gel 60 (0.063–0.200 μm, Merck) was used for column chromatography. The synthesis of 1-HMP was performed as previously described [9].

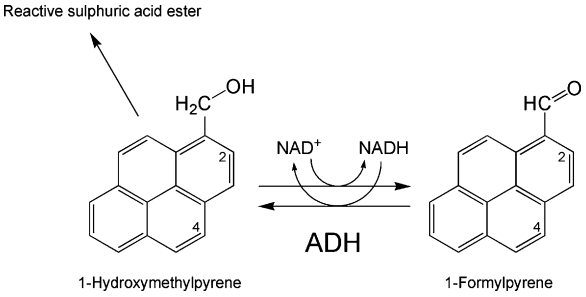

Fig. 1 – Scheme of the ADH-catalyzed oxidation of 1-HMP, a reaction competing with its bioactivation to an electrophilically reactive sulphuric acid ester. The positions of the substituents in the two possible positional isomers are indicated. All three isomers were investigated in the present study.

2.2.1. Synthesis of 2-hydroxymethylpyrene (2-HMP)

A solution of 1.3 g (5 mmol) 2-pyrenecarboxylic acid methyl ester [16] in 35 ml anhydrous tetrahydrofuran was added dropwise to a suspension of 0.58 g (15 mmol) of $LiAlH_4$ in 15 ml anhydrous tetrahydrofuran. After stirring at room temperature for 18 h, a concentrated solution of NaCl in water (15 ml) was cautiously added. Then, 10 ml of glacial acetic acid was added to dissolve the aluminium salts. The product was extracted with ethyl acetate, washed with a saturated solution of $NaHCO_3$ in water, dried, and concentrated. Chromatography on silica gel (CH_2Cl_2/MeOH 95/5) provided 0.43 g (37% yield) of 2-HMP as white crystals; mp 167–168 °C (lit. [17] 168–169 °C); UV (CH_3OH) λ_{max} (nm): ε [cm^2 $mmol^{-1}$] 235 (133,100), 244 (231,200), 253 (66,200), 263 (105,800), 274 (151,600), 306 (37,600), 320 (76,100), 335 (122,000); ^1H NMR (400 MHz, $CDCl_3$) δ [ppm] 7.99 (d, 2, $H_{6,8}$, $J_{6,7} = J_{7,8} = 7.6$ Hz), 7.97 (s, 2, $H_{1,3}$), 7.87 (d, 4, $H_{4,5,9,10}$, $J_{4,5} = J_{9,10} = 3.5$ Hz), 7.83 (p–t, 1, H_7, $J_{7,6} = J_{7,8} = 7.6$ Hz), 4.95 (s, 2, benzylic CH_2).

2.2.2. Synthesis of 2-formylpyrene (2-FP)

A total of 2.9 g (7.6 mmol) of pyridinium dichromate was added in small portions at room temperature to a solution of 1.16 g (5 mmol) of 2-HMP in 70 ml of dichloromethane. After stirring for 18 h, the mixture was filtrated, and the filtrate was concentrated. Chromatography on silica gel (CH_2Cl_2) provided 0.70 g (61% yield) of 2-FP as white crystals; mp 153° (lit. [17] 153–154 °C); UV (CH_3OH) λ_{max} (nm): ε [cm^2 $mmol^{-1}$] 244 (68,800), 274 (106,000), 307 (18,900), 321 (34,800), 336 (60,500); ^1H NMR (400 MHz, $CDCl_3$) δ [ppm] 10.44 (s, 1, –CHO), 8.63 (s, 2, $H_{1,3}$), 8.24 (d, 2, $H_{6,8}$, $J_{6,7} = J_{7,8} = 7.6$ Hz), 8.08–8.17 (m, 5, $H_{4,5,7,9,10}$).

2.2.3. Synthesis of 4-pyrenecarboxylic acid

A sample of 2.9 g (18 mmol) Br_2 was added dropwise at 0 °C to a stirred solution of 2.6 g (65 mmol) NaOH in 12 ml of water. The solution was heated to 35 °C, and a solution of 1.0 g (4.1 mmol) of 4-acetylpyrene [18,19] in 10 ml of dioxane was added dropwise. Excess Br_2 was destroyed by addition of $NaHSO_3$ (40% solution in H_2O). The mixture was then diluted with 100 ml of water and the dioxane was distilled off. The yellow precipitate was dissolved in 1000 ml of 5% NaOH in water, the solution was filtrated and acidified with concentrated

hydrochloric acid. The precipitated product was filtrated, washed with water, and dried. Crystallization from chlorobenzene gave 0.886 g (88% yield) of 4-pyrenecarboxylic acid as yellow crystals; mp 274–275 °C (lit. [18] 275.5–276 °C); UV (CH_3OH) λ_{max} (nm): ε [$cm^2\ mmol^{-1}$] 205 (32,000), 242 (57,300), 266 (18,700), 276 (31,400), 310 (9,500), 323 (18,200), 339 (26,700); ^1H NMR (400 MHZ, DMSO-d_6) δ [ppm] 13.22 (s, 1, –COO*H*), 9.09 (dd, 1, H_3, $J_{2,3}$ = 7.8 Hz, $J_{1,3}$ = 0.7 Hz), 8.79 (s, 1, H_5) 8.35 (d, 1, H_1, $J_{1,2}$ = 7.4 Hz), 8.29 (dd, 1, H_6, $J_{6,7}$ = 7.6 Hz, $J_{6,8}$ = 0.8 Hz), 8.24 (dd, 1, H_8, $J_{7,8}$ = 7.6 Hz), 8.09 (AB-system, 2, $H_{9,10}$, $J_{9,10}$ = 9.0 Hz), 7.99–8.09 (m, 2, $H_{2,7}$), 8.03 (p–t, 1, H_7).

2.2.4. *Synthesis of 4-hydroxymethylpyrene (4-HMP)*

A solution of 0.88 g (3.5 mmol) of 4-pyrenecarboxylic acid in 35 ml anhydrous tetrahydrofuran was added dropwise to a suspension of 0.40 g (11 mmol) of $LiAlH_4$ in 15 ml anhydrous tetrahydrofuran. After stirring at room temperature for 18 h, a concentrated solution of NaCl in water (10 ml) was cautiously added to the mixture. Glacial acetic acid (15 ml) was then added to dissolve the aluminium salts. The product was extracted with ethyl acetate, washed with a saturated solution of $NaHCO_3$ in water, dried, and concentrated. Chromatography on silica gel (CH_2Cl_2) provided 0.80 g (84% yield) of 4-HMP as pale yellow crystals; mp 151–152 °C; UV (CH_3OH) λ_{max} (nm): ε [$cm^2\ mmol^{-1}$] 242 (63,300), 264 (23,500), 275 (42,100), 307 (10,600), 320 (25,900), 336 (40,100); ^1H NMR (500 MHZ, $CDCl_3$) δ [ppm] 8.43 (d, 1, H_3, $J_{2,3}$ = 7.8 Hz), 8.24 (d, 1, H_1, $J_{1,2}$ = 7.8 Hz), 8.21 (d, 1, H_6, $J_{6,7}$ = 7.6 Hz), 8.20 (d, 1, H_8, $J_{7,8}$ = 7.6 Hz), 8.16 (s, 1, H_5), 8.11 (s, 2, $H_{9,10}$), 8.07 (p–t, 1, H_2), 8.03 (p–t, 1, H_7), 5.39 (s, 2, benzylic CH_2).

2.2.5. *Synthesis of 4-formylpyrene (4-FP)*

A total 2.9 g (7.6 mmol) of pyridinium dichromate was added in small portions to a solution of 1.16 g (5 mmol) of 4-HMP in 70 ml of dichloromethane at room temperature. After stirring for 18 h, the mixture was filtrated, and the filtrate was concentrated. Chromatography on silica gel (CH_2Cl_2) provided 0.89 g (77% yield) of 4-FP as yellow crystals; mp 177–178 °C (177–179 °C [16]); UV (CH_3OH) λ_{max} (nm): ε [$cm^2\ mmol^{-1}$] 210 (29,300), 223 (27,800), 242 (44,700), 275 (16,900), 311 (10,000), 321 (7,100), 337 (10,600), 355 (9,100), 389 (5,300); ^1H NMR (400 MHz, $CDCl_3$) δ [ppm] 10.43 (s, 1, –C*H*O), 9.52 (dd, 1, H_3, $J_{2,3}$ = 8.0 Hz, $J_{1,3}$ = 0.9 Hz) 8.49 (s, 1, H_5), 8.23 (d, 2, H $_{9,10}$, $J_{9,10}$ = 7.8 Hz), 8.16 (dd, 1, H_1, $J_{1,2}$ = 7.7 Hz), 7.94–8.05 (m, 4, $H_{2,6,7,8}$).

2.3. *Bacterial expression of human ADH2*

ADH2 cDNA was isolated using reverse transcription (RT) polymerase chain reaction (PCR) from a human liver sample. Total RNA was isolated with RNeasy mini Kit from Qiagen (Hilden, Germany). Two micrograms of total RNA were subjected to RT with the DuraScript First Strand Synthesis Kit (Sigma–Aldrich, Taufkirchen, Germany) according to the manufacturer's instructions. Two microliters of the RT reaction product was used for amplification of ADH2 cDNA using 2 units *Pfu* DNA polymerase (Promega, Mannheim, Germany) in a final volume of 50 μl according to the manufacturer's recommendations. The forward primer, 5′-ACAGTTTCCCAAAGAACCATGGGCACCAAG, introduced an *Nco*I restriction site at the position of the translation start codon of ADH2. The reverse primer, 5′-ACCAGGAAGCTTCACATTCAATCAGATAGTTATTC, introduced a *Hin*dIII restriction site in the 3′-flanking region. The reaction conditions for PCR were: 2 min at 95 °C for initial denaturing; 30 s at 94 °C for the later denaturing steps, 45 s at 57 °C for annealing, and 3 min at 72 °C for the elongation (40 cycles); and a final elongation step at 72 °C for 10 min.

The amplified ADH2 cDNA was cloned into the prokaryotic expression vector pKK233-2 (Clontech, Mountain View, USA) utilizing the 5′ *Nco*I and the 3′ *Hin*dIII restriction sites. Sequencing confirmed that the cloned cDNA was identical (with the exception of a silent nucleotide exchange, A653G) to that reported in the database for human ADH2 (GenBank accession no. BC022319). This sequence contains G in the polymorphic position 925 (A or G, encoding ^{308}Ile or ^{308}Val, respectively), the variant that is predominating in the Swedish population [20]. The plasmid was initially transfected into *Escherichia coli* XL-1 blue (Stratagene) and then adapted to the restriction enzymes of *S. typhimurium* LT2 by passaging through the restriction-deficient, but methylation-proficient *S. typhimurium* strain LB5000 [21], before transforming the Ames tester strain TA1538 [22]. The resulting recombinant strain was termed TA1538-hADH2. Transformation of the strain TA100, which already contains an ampicillin resistance marker [22], was performed in an analogous manner after subcloning the ADH2 cDNA into the expression vector pKN, a derivative of pKK233-2 encoding a neomycin resistance marker instead of an ampicillin resistance marker [23], utilizing the 5′ *Sal*I and 3′ *Hin*dIII restriction sites. The resulting recombinant strain was termed TA100-hADH2.

Bacterial expression of the other human ADH enzymes was performed analogously (Table 1). The names of the resulting strains are composed of the designation of the recipient strain (TA1538 and TA100) and the expressed enzyme (hADH1A, hADH1B, hADH1C hADH3 and hADH4).

2.4. *Purification of ADH2*

Cytosolic fraction of the transformed *S. typhimurium* strain TA100-ADH2 was used as the source for the purification of ADH2. The cytosolic fraction was prepared as described previously [24] using 10 mM Tris/HCl buffer (pH 8.0) containing 1 mM dithiothreitol as the homogenisation medium. The protein was purified on a FPLC unit (Biorad, Munich, Germany) with the following specifications: MV-6 6-port injection valve, EP-1 Econo Pump, Econo-Pac Cartridge HighQ (5 ml), EM-1 Econo UV Monitor, and EG-1 Econo Gradient Monitor. Column and eluents were maintained at 4 °C. After conditioning of the column with 10 mM Tris/HCl (pH 8.0), 5 ml cytosolic fraction (10 mg protein) was loaded. Proteins were eluted, at a flow rate of 1 ml/min, with 10 mM Tris/HCl (pH 8.0) for 60 min and then for another 60 min with the same buffer containing 0.5 M NaCl. Fractionation was guided by protein peaks monitored spectrometrically at 280 nm. The fractions were concentrated to a final volume of 200–400 μl using AmiconUltra Centrifugal Filter Devises 30,000 MWCO (Millipore, Carrigtwohill, Ireland) and were analyzed by sodium dodecyl sulphate polyacrylamide gel electrophoresis (SDS-PAGE) [25] and subsequent Coomassie blue staining. Fractions were also assayed for ADH activity (Section 2.5). To distinguish endogenous ADH activity

Table 1 – Human ADH cDNA sequences cloned into the pKK233-2 expression vector

ADH	GenBank accession number	Amplified coding sequence (nucleotides)	Primer sequences used for the amplification
1A	NM000667	4-1128	5′-CTC CTG GTC TGC AGA GAA GAC AGA ATC AAC (forward, 1st PCR) 5′-CAA TTT CCA TTT CTT TGG AAA GCC CCC AAA (backward, 1st PCR) 5′-AGC ACA GCA GGA AAA GTA AT (forward, 2nd PCR) 5′-CAT CTG TAA *AGC TTC* AAA AC (backward, 2nd PCR)
1B	BC033009	4-1128	5′-AAT CCA CAA AGA CTC ACA GTC TGC TGG TGG (forward, 1st PCR) 5′-TAT TTT TCC TCA ATG GCA AAG GTG ACA CAG (backward, 1st PCR) 5′-AGC ACA GCA GGA AAA GTA ATC AAA TGC AAA G (forward, 2nd PCR) 5′-GCA TCT CTA *AAG CTT* CAA AAC GTC AGG ACG (backward 2nd PCR)
1C	NM000669	4-1128	5′-CAG AGA AGA AAT CCA CAA GTA CTC ACC AGC (forward, 1st PCR) 5′-TCA ATT TCC ATT TCT TTG GAA AGC TCC CAC (backward, 1st PCR) 5′-AGC ACA GCA GGA AAA GTA ATC AAA TGC AAA G (forward, 2nd PCR) 5′-GCA TCT CTA *AAG CTT* CAA AAC GTC AGG ACG (backward, 2nd PCR)
2	BC022319	1-1179	5′-ACA GTT TCC CAA AGA *ACC ATG* GGC ACC AAG (forward) 5′-ACC AGG *AAG CTT* CAC ATT CAA TCA GAT AGT ATT C (backward)
3	BC014665	1-1125	5′-GCC GAC CAG AAT CCG TGA *CCA TGG* CGA ACG (forward) 5′-ATT ATT TAA *GCT TTT* GAA TTA AAT CTT TAC A (backward)
4	X76342	4-1125	5′-GGC ACT GCT GGA AAA GTT ATT AAA TGC AAA GCA GCT GTG CTT (forward) 5′-GAC AAC ACA *AGC TTC* CTG CCA CTT TGG ATC (backward)

Due to the similarity (>90%) among the various ADH1 sequences, nested PCRs were required for obtaining the individual ADH1 forms. The final amplification products were inserted into the vector using the *Nco*I (CCATGG) and *Hind*III (AAGCTT) restriction sites (italicized when introduced with the primers). For inserting ADH1A, 1B, 1C and 4, the *Nco*I-digested pKK233-2 plasmid was treated with Klenow fragment in order to obtain blunt ends concluding with the start codon ATG (which therefore was not included in the amplified cDNA sequence). In all cases, the resulting vector encoded the correct amino acid sequence of the corresponding ADH with start and stop codons in the right positions. The cloning and expression of ADH2 are presented in detail in Section 2.

from that produced by the cDNA-expressed human enzyme, the same separation and analyses procedures were performed using cytosol from the untransformed strain TA100 as the starting material.

Protein concentrations were determined using the BCA Protein Assay Kit (Pierce, Rockford, USA).

2.5. *Measurement of enzyme activities*

Three different assays were used for determining ADH2 activity towards various substrates: (a) by continuous spectrometric monitoring of the reaction at 340 nm or 360 nm (production/consumption of NADH, corrected in the case of the pyrene derivatives for differences in absorption between the alcohol and the aldehyde); (b) measurement of the NADH present a given time point using an HPLC/UV detection method; and (c) as assay b but measuring the other product formed, the aldehyde (only used for pyrene derivatives).

Cofactor concentrations and buffers used in the incubations were the same for all three assay systems. The oxidation reaction was performed in 0.1 M glycine/NaOH buffer (pH 10.0) with 1.25 mM NAD^+ as cofactor and the reduction reaction in 0.1 sodium phosphate buffer (pH 7.5) with 0.25 mM NADH as cofactor. The pyrene derivatives had to be delivered in an organic solvent, such as DMSO. Depending on the individual pyrene derivative and its concentration, up to 10% DMSO was required in the assay to obtain an optically clear solution. When BSA (0.33%) was added, the DMSO concentration could be reduced to 0.33%. Incubations were conducted at ambient temperature (21–23 °C) in the continuous spectrometric assay or at 37 °C in the endpoint assays, unless specified otherwise.

2.5.1. *Continuous spectrometric assay*

Continuous reaction monitoring has obvious advantages. For example, a deviation from linearity with time is immediately recognized. Likewise levels of enzyme, substrate or modulator can quickly be optimised, since the result is immediately available. Biochemical reactions involving the co-substrate NAD(P)(H) are commonly monitored using the fact that only the reduced form absorbs light in the 340–360 nm range. However, pyrene derivatives exhibit high absorbance in the same wavelength range. The spectra of the HMPs and the corresponding FPs differ and are also affected by the presence or absence of BSA. Thus, for calculating reaction rates, one has to take into account the sum of the absorption changes due to the formation or utilization of NADH, the formation or disappearance of FP, and the disappearance or formation of the HMP. We have monitored most reactions at 360 nm. At this wavelength, the extinction coefficients (ε in cm^2 $mmol^{-1}$ units were: 3700 for of NADH and 1100 for 1-HMP under all conditions; 13,500 and 28,500 for 1-FP in the absence and presence of BSA (0.33%), respectively; the corresponding values were 1000 and 100 for 4-HMP; 9800 and 12,600 for 4-FP; 400 and 130 for 2-HMP; 5900 and 230 for 2-FP (with the last compound, this value was dependent on the buffer used; the values given refer to the media used for the reduction reaction). Oxidation of 2-HMP was monitored at 340 nm, using the following ε values: 6200 for NADH; 12,000 and 29,420 for 2-HMP in the absence and presence of BSA, and 11,300 and 34,870 for 2-FP in the absence and presence of BSA. The correctness of results of the continuous assay was examined in exemplary cases using the endpoint assays (all conducted at ambient temperature).

2.5.2. *Endpoint assay with determination of NADH by HPLC*
After the incubation (5 min unless specified otherwise), the reaction was stopped by heating to 95 °C for 5 min. It was verified that no NADH was destroyed by this short heat treatment. Insoluble components were then sedimented by centrifugation at 23,000 × *g* for 10 min. The supernatant was subjected to HPLC analysis (automatic sample injector ASI-100, HPLC pump P580 and column oven STH585 from Dionex, Idstein, Germany). An aliquot of 10 μl was injected into a hydrosphere C18 column (5 μm, 4 mm × 150 mm, YMC, Schermbeck, Germany). The elution was conducted isocratically with a mixture of 80% eluent E1 (20 mM KH_2PO_4, 2 mM tetrabutylammonium hydrogensulphate, pH 3.9) and 20% eluent E2 (methanol) at a flow rate of 0.7 ml/min with a column temperature of 40 °C. The NADH formed was detected at 340 nm in a UV detector (UV-970, Jasco, Gross-Umstadt, Germany) and quantified using external standards. In this assay, an individual reaction product is detected with high specificity and sensitivity.

2.5.3. *Endpoint assay with determination of 1-FP by HPLC*
The assays presented in the preceding sections are only useful when a single substrate is used, but not when the competition between different substrates is the object of the investigation. In that case, the product of interest (1-FP) has to be analysed directly. The enzymatic reaction was carried out and stopped as described in the preceding paragraph. The 1-FP formed was detected by HPLC with a Waters 2695 Separations Module (Waters, Eschborn, Germany) equipped with a 5-μm Supelcosil LC-18 column (25 mm × 4.6 mm) (Sigma–Aldrich, Taufkirchen, Germany) using a Waters 474 Fluorescence Detector (excitation: 396 nm, emission: 450 nm). HPLC conditions were as followed: HPLC was started with 10% acetonitrile and 10% methanol in water, pH 2.3 (adjusted with phosphoric acid) as the eluent. A linear gradient up to 35% acetonitrile and 35% methanol was used in the initial 5 min. Chromatography was continued using these concentrations until 20 min, followed by a linear gradient back to 10% acetonitrile and 10% methanol for the next 5 min, and continued with these concentrations until 30 min. 1-FP eluted from the column with a retention time of 19.5 min and was quantified using external standards.

More than 80% of 1-FP (20 μM) added to a solution of 0.33% BSA was recovered after an incubation period of 1 h at room temperature. Since the incubation time for studying the formation of 1-FP from 1-HMP was much shorter (5 min), no corrections were made.

2.6. Kinetic and inhibition studies

For determining the apparent V_{max} and K_m values, the reaction rate (v) was measured using various concentrations of the substrate S. The data points were fitted to the Michaelis–Menten equation $v = (V_{max}\ [S])/(K_m + [S])$ using non-linear regression analysis (SigmaPlot 8.02, SPSS Science Software), to give estimates of the kinetic constants (±S.E.).

For investigating inhibition kinetics, the concentrations of the inhibitor and the substrate were varied. 4-Methylpyrazole and cimetidine were delivered in reaction buffer. Daidzein was delivered in DMSO (final incremental concentration 1%, also added in corresponding controls). The method of Dixon [26] was used to determine apparent K_i values: a vertical straight line is dropped from the intersect of the lines representing results obtained at a individual concentration of the inhibitor; the value indicated on the *x*-axis by this vertical line is equal to $-K_i$.

Molecular turnover rates were calculated from V_{max} (at ambient temperature for the most favourable solubilizing regimen) using a molecular mass of 40,220 Da for the ADH subunit and a purity of 90% of the purified enzyme.

3. Results

3.1. Oxidation of HMPs in cytosolic preparations from bacteria expressing individual human ADH forms

Control cytosol prepared from untransformed strain TA100 showed endogenous ADH activity using HMPs as the substrates. Activity with all three isomers was enhanced (1.9–7.3-fold) when ADH2 was expressed (Table 2). Activity towards 2-HMP, but not the other isomers, was also enhanced when ADH3 or ADH4 was expressed (5.1- and 5.6-fold, respectively). Activities were hardly changed in TA100-hADH1C compared to TA100 cytosol. In all remaining cases, the expression of a human ADH tended to decrease ADH activity towards HMPs compared to control cytosol. We have not explored the underlying mechanism, which might – for example – involve down-regulation of endogenous ADH in the presence of certain heterologous ADHs.

Levels of ADH1B, 1C, 3 and 4 in recombinant strains were similar to those of ADH2 in TA100-hADH2 (differing by a factor of ≤1.35). ADH1A was expressed at a markedly lower level than ADH2 (by a factor of 8), but this protein decreased rather than increased the activity towards HMP. Based on these findings, we expect that ADH2 may play a prominent role in the sequestration of benzylic alcohols and the prevention of their SULT-mediated toxification in human tissues.

3.2. Partial purification of ADH2

Before appropriate kinetic analysis with cDNA-expressed human ADH2 could be conducted, it was necessary to remove the endogenous ADH enzyme(s) present in *Salmonella* cytosol. Various mammalian ADHs show unusually weak interactions with anion exchange materials [20]. Indeed, in our FPLC procedure, ADH activity was eluted in the flow-through front with the low-salt eluent (starting with 5 ml of the eluate up to about 15 ml); later fractions of the low-salt mobile phase contained no ADH activity. However, ADH activity was again eluted – together with the bulk of the proteins – by the high-salt mobile phase. This later activity peak was also seen when cytosol from untransformed bacteria was chromatographed, indicating that it represented endogenous ADH. By contrast, the front peak was only seen with cytosol from recombinant bacteria, indicating that it constituted human ADH2 free from endogenous bacterial ADH. Fractions I and II representing 5–9 and 10–15 ml, respectively, were then analysed by SDS-PAGE and Coomassie blue staining. Both fractions contained a major protein band of approximately 40 kDa, as estimated from its electrophoretic mobility. This value agrees with the molecular

Table 2 – Oxidation of HMPs by cytosolic preparations from *Salmonella typhimurium* strains engineered for expression of human ADHs

Human ADH expressed	ADH expression level (μg ADH protein/mg cytosolic protein)[a]	Activity (nmol/[min mg])		
		1-HMP	2-HMP	4-HMP
None	–	3.3 ± 0.1	1.8 ± 0.0	0.6 ± 0.0
ADH1A	2.5	1.4 ± 0.1	0.7 ± 0.0	0.2 ± 0.0
ADH1B	16	2.0 ± 0.1	1.3 ± 0.1	0.3 ± 0.0
ADH1C	14	4.4 ± 0.0	1.9 ± 0.0	0.6 ± 0.1
ADH2	20	6.1 ± 0.3	13.1 ± 0.0	4.5 ± 0.1
ADH3	27	2.0 ± 0.0	9.2 ± 0.4	0.3 ± 0.0
ADH4	16	2.4 ± 0.2	10.1 ± 0.6	0.3 ± 0.1

Human ADHs were expressed in *S. typhimurium* TA100. Cytosolic fraction (200 μg protein), substrate (100 μM) and NAD^+ (1.25 mM) were incubated in a total volume of 1 ml at 37 °C for 20 min. The final concentration of the delivering solvent DMSO was 10%. No BSA was used. The NADH formed was determined by the HPLC/UV method. Values are means ± S.D. of two incubations. Formation of NADH was not detected (<0.1 nmol/min/mg) when no substrate was added.

[a] Levels of human ADH proteins in the cytosolic fraction were estimated from immunoblots using nearly homogeneous inclusion bodies as standards and antisera raised against the inclusion bodies as probes (Kollock and Glatt, manuscript in preparation). The procedure is analogous to that used for quantifying cDNA-expressed human SULTs [39].

mass of the ADH2 peptide unit deduced from its cDNA sequence (40,220 Da). This 40-kDa band contributed >90% and ~75% of the protein detected by the Coomassie-staining in fractions I and II, respectively. The specific activities, using 33 mM ethanol as the substrate, amounted to 410 and 370 nmol/(min mg) protein. These values were about 20- and 22-fold higher than the net ADH2 activity in TA100-hADH2 cytosol (*i.e.* after subtracting the activity detected in cytosol from the untransformed control strain, TA100). Due to its higher purity, fraction I was used for all subsequent investigations.

3.3. *Effect of solubilizers for pyrene derivatives on ADH activities with reference substrates*

Since alcohols and aldehydes of alk-PAHs are very poorly soluble in aqueous media, they have to be delivered in a water-miscible organic solvent such as DMSO. When the concentration of the test compound in the delivering solvent was too high, it precipitated at the addition site in the incubation. This effect could be prevented by adding BSA to the medium. However, solubilizers may affect the catalytic activities of enzymes. Indeed, it has been reported DMSO is a moderately potent inhibitor of various ADH forms [27,28]. Human ADH2 had not yet been investigated in this regard. Therefore, we studied the influence of DMSO and BSA on ADH2 activity using substrates that pose no solubility problems, ethanol and acetaldehyde. DMSO inhibited the oxidation as well as the reduction reaction. As seen from Lineweaver–Burk plots, inhibition was uncompetitive for the oxidation of ethanol (Fig. 2A), and of the mixed type, with a preponderance of the competitive component, for the reduction of acetaldehyde (Fig. 2B). The presence of BSA did not affect the oxidation reaction (data not shown), but decreased the aldehyde

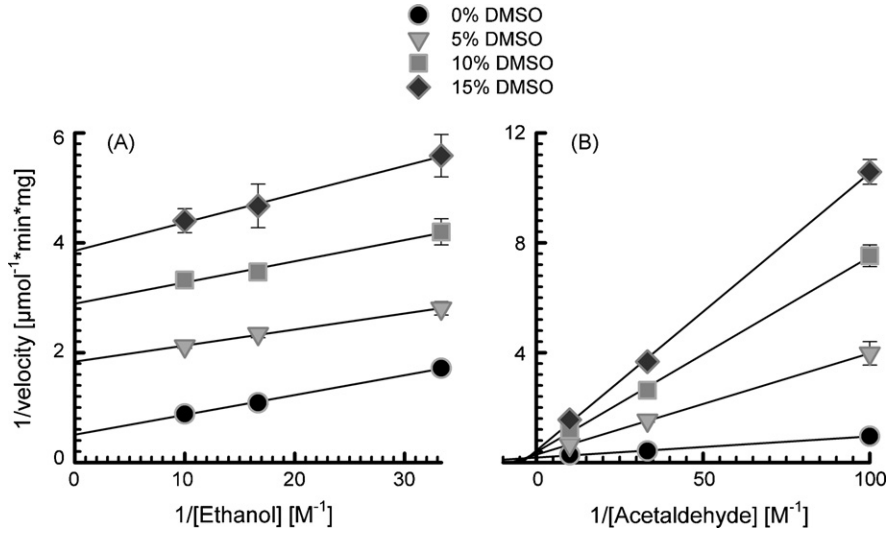

Fig. 2 – Lineweaver–Burk plots for the oxidation of ethanol (A) and the reduction of acetaldehyde (B) by ADH2 in the presence of varying concentrations of DMSO. Reactions were conducted at ambient temperature. They were continuously monitored in a spectrometer (measuring the production or utilization of NADH at 340 nm). Values are means and range of two determinations.

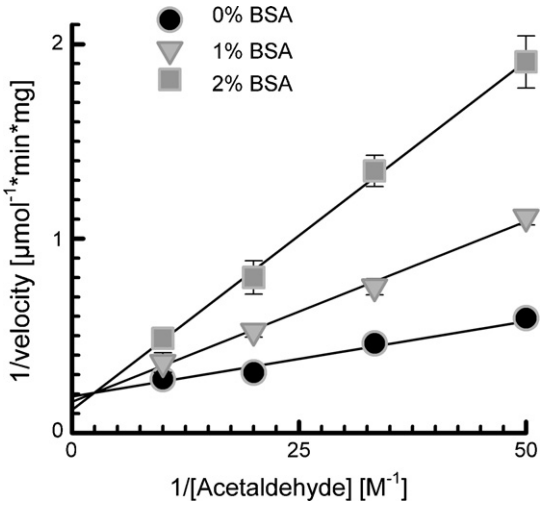

Fig. 3 – Lineweaver–Burk plot for the reduction of acetaldehyde by ADH2 in the presence of varying concentrations of BSA. The reaction in the other direction, the oxidation of ethanol, was unaffected in the presence of BSA. Reactions were conducted at ambient temperature. They were continuously monitored in a spectrometer (measuring the production or utilization of NADH at 340 nm). Values are means and range of two determinations.

reduction in a competitive mode with a slight activating component at high substrate concentrations (Fig. 3). Competition inhibition may not require direct interaction of BSA with ADH2, but alternatively could also result from reversible binding of the substrate to BSA.

3.4. *Oxidation of HMP isomers and reduction of FP isomers by ADH2*

Two different regimens were used for delivering the substrates. In the first regimen, the substrates were added using a relatively high amount of DMSO (final concentration up to 10% for the least soluble compounds, the FPs); in the second regimen, a lower level of DMSO (0.33%) was used in combination with the presence of BSA (0.33%) in the incubation mixture. The kinetic constants differed between these conditions. The apparent K_m values as well as the V_{max} values were increased with the second protocol (Table 3). The effect on the apparent K_m values was not surprising, as BSA reduces the free concentration of the pyrene derivatives by reversible binding. However, the bound substrate may act as a deposit to rapidly replenish the free form eliminated by ADH. This mechanism and the reduced level of the inhibitory solvent DMSO explain the increases in V_{max} values in the second protocol. Humans are normally exposed to very low levels of methylpyrenes and their benzylic oxidation products. Under these conditions, the catalytic efficiency (V_{max}/K_m) is the most relevant kinetic parameter. For all methylpyrene derivatives studied, this value was somewhat lower in the second regimen (presence of BSA) than in the first regimen (increased level of DMSO). It is likely that it would be even higher in the absence of both solubilizers, the conditions used for studying the biotransformation of the reference substrates ethanol and acetaldehyde. Nevertheless, the catalytic efficiency of ADH2 was greater for the pyrene derivatives than for the reference substrates by a factor of up to 10,000 (oxidation of 2-HMP using regimen 1, compared to the oxidation of ethanol). The high catalytic efficiency with the methylpyrene derivatives was primarily produced by low K_m values. Nevertheless, the V_{max} values for 2-HMP (both regimens) and 2-FP (low-DMSO regimen) also exceeded the V_{max} values for ethanol and acetaldehyde, respectively. The calculated molecular turnover rates [nmol substrate metabolized per nmol enzyme subunit per second] at V_{max} amounted to 1.0, 0.5, 3.5 and 1.3 for ethanol, 1-HMP, 2-HMP and 4-HMP, respectively, and 3.3, 0.3, 4.8 and 0.2 for the corresponding reverse reaction (in the presence of BSA for the methylpyrene derivatives).

For all substrate pairs and conditions, the catalytic efficiencies of the reverse reaction (reduction of the aldehyde) were somewhat higher than for the forward reaction (oxidation of the alcohol).

Table 3 – Kinetics of the oxidation of HMPs compared to the reference substrate ethanol and of the corresponding reverse reactions by of ADH2

Substrate	Solubilizer[a]	Oxidation of the alcohol			Reduction of the aldehyde		
		V_{max} (nmol/[min mg])	K_m (µM)	V_{max}/K_m (ml/[min mg])	V_{max} (nmol/[min mg])	K_m (µM)	V_{max}/K_m (ml/[min mg])
Ethanol/ acetaldehyde	None	1350 ± 80	33000 ± 4000	0.04	4400 ± 300	26000 ± 4000	0.2
1-HMP/1-FP	DMSO-high	600 ± 40	76 ± 7	8	140 ± 7	12 ± 2	12
	DMSO-low, BSA	680 ± 140	350 ± 90	2	460 ± 30	95 ± 8	5
2-HMP/2-FP	DMSO-high	1800 ± 100	4.4 ± 0.7	409	1210 ± 110	2.9 ± 0.2	417
	DMSO-low, BSA	4700 ± 700	80 ± 20	59	6400 ± 200	29 ± 2	221
4-HMP/4-FP	DMSO-high	860 ± 110	40 ± 10	22	189 ± 4	3.8 ± 0.3	50
	DMSO-low, BSA	1770 ± 220	240 ± 40	7	268 ± 5	10.2 ± 0.5	26

Reactions were conducted at ambient temperatures. They were continuously monitored by UV spectrometry (at λ = 340 or 360 nm).
[a] The final concentrations of the solubilizers were 0.33% DMSO and 0.33% BSA (DMSO-low, BSA) or the minimal level of DMSO required to keep the incubation mixture over the entire concentration range used for the corresponding compound, 2% for 2-HMP, 6% for 1-HMP and 4-HMP, and 10% for all FP isomers.

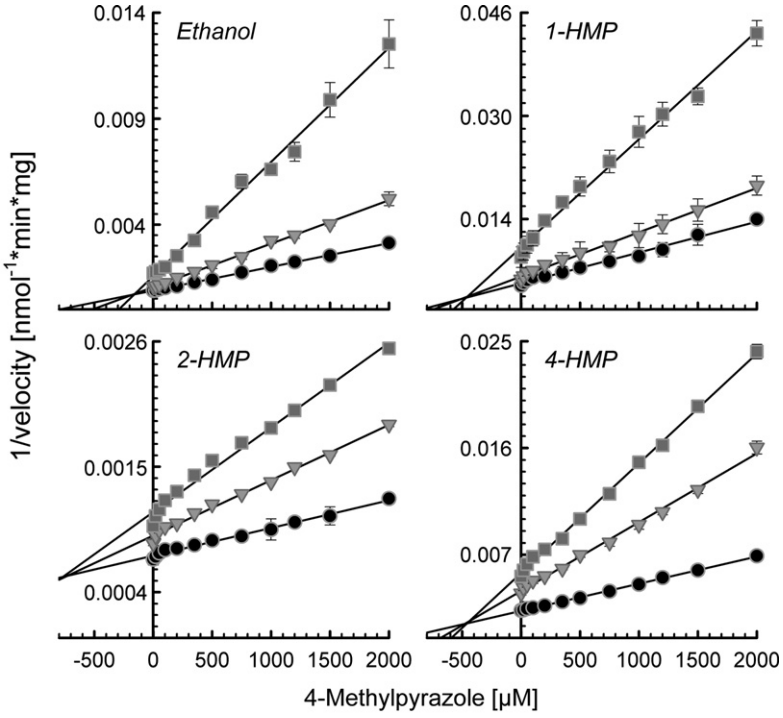

Fig. 4 – Dixon plots of the ADH2-catalyzed oxidation of ethanol and HMP isomers in the presence of varying concentrations of 4-methylpyrazole. The substrates were used at the following concentrations—ethanol: 100 mM (●), 60 mM (▽) and 30 mM (■); 1-HMP: 60 μM, (●), 40 μM (▽) and 20 μM (■); 2-HMP: 20 μM (●), 10 μM (▽) and 5 μM (■); 4-HMP: 40 μM (●), 20 μM (▽) and 10 μM (■). Solubilizing regimen 1 (6% DMSO) was used with the HMPs. The reactions were carried out at ambient temperature. They were continuously monitored by UV spectrometry (at λ = 340 or 360 nm). Values are means and range of two determinations.

3.5. *Inhibition of ADH2 catalyzed oxidation of HMP isomers*

The ADH2-mediated oxidation of the HMP isomers was clearly inhibited in the presence of 4-methylpyrazole (Fig. 4). The K_i values were 480 ± 40 μM with the substrate 1-HMP, 770 ± 50 μM with 2-HMP and 460 ± 30 μM with 4-HMP. These values were 2.5–4.5-fold higher than the apparent K_i value determined using ethanol as the substrate 170 ± 20 μM (Fig. 4, upper left panel).

Inhibition of the ADH2-catalyzed oxidation of 1-HMP was also studied using the known ADH inhibitors daidzein [29] and cimetidine [30] and compared with the inhibition of ethanol oxidation by these compounds (Fig. 5). The apparent K_i value for daidzein was similar with both substrates used: 58 ± 2 μM with 1-HMP and 51 ± 2 μM with ethanol (Fig. 5, left panels). By contrast, the inhibition by cimetidine was stronger for the oxidation of ethanol (K_i = 900 ± 200 μM) than for the oxidation of 1-HMP (K_i = 4400 ± 400 μM) (Fig. 5, right panels).

Ethanol inhibited the ADH2-mediated oxidation of 1-HMP with an apparent K_i value of 38 ± 2 mM (Fig. 6). This K_i value is similar to the K_m value for the ADH2-mediated oxidation of ethanol (33 mM, Table 3).

4. Discussion

Concurrent exposure to ethanol or 4-methylpyrazole led to a dramatic increase in the bioactivation of 1-HMP in rats in a preceding study [12]. Levels of 1-methylpyrenyl DNA adducts were increased up to 200-fold in liver, lungs and kidneys. Likewise, serum levels of 1-sulphooxymethylpyrene and excretion of 1-methylpyrenyl mercapturic acid were elevated. This interaction study had been conducted after observing that free and conjugated carboxylic acids were the predominating metabolites of 1-HMP excreted in urine and faeces. Evidently, oxidation of the hydroxyl group would prevent its sulpho conjugation, *i.e.* the bioactivation. Since we considered ADHs as the primary candidate enzymes to mediate the first oxidation step of 1-HMP, we had used ethanol (a competing ADH substrate) and 4-methylpyrazole (an ADH inhibitor) in the animal studies. The strongly enhanced bioactivation of 1-HMP in co-treated animals corroborated our hypothesis on an involvement of ADHs. At this stage it became important to identify the ADH forms involved in order to specify the mechanism underlying the interaction and to facilitate the detection of other interacting factors. For the purpose of elucidating the results of the animal experiment it would have been optimal to study rat ADHs. However, since effects and interactions occurring in humans are of much higher interest, we cloned and studied the ADHs from this species. We found that human ADH2 shows particular high catalytic activity towards all three possible isomers of HMP. Previously, it was found that ADH2 prefers aromatic and large aliphatic alcohols [31]. The aromatic alcohols studied at that time were benzyl alcohol and 3-phenyl-1-propanol, molecules containing a single

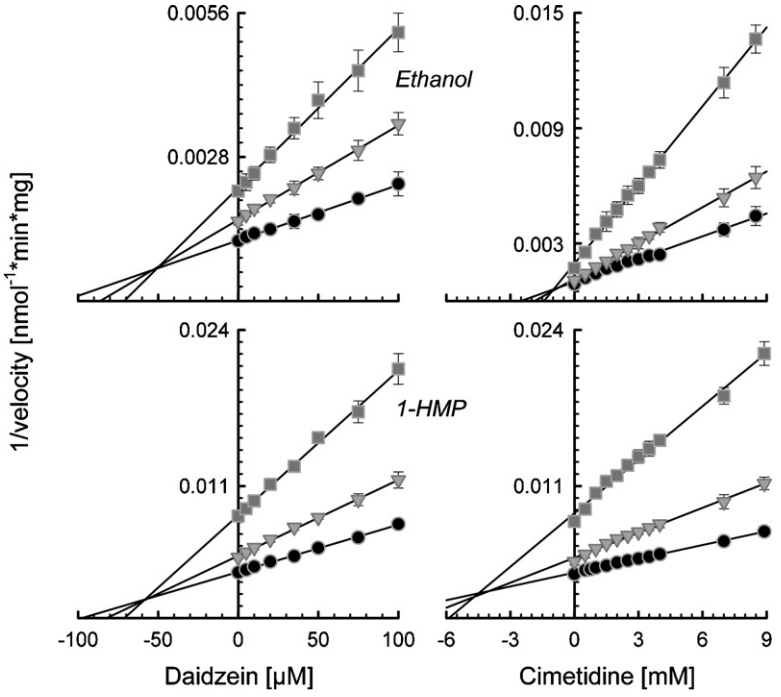

Fig. 5 – Dixon plots of the ADH2-catalyzed oxidation of ethanol (upper panels) and 1-HMP (lower panels) in the presence of varying concentrations of daidzein (left panels) and cimetidine (right panels). The substrates were used at the following concentrations—ethanol: 100 mM (●), 60 mM (▽) and 30 mM (■); 1-HMP: 60 μM (●), 40 μM (▽) and 20 μM (■). Solubilizing regimen 1 (6% DMSO) was used with 1-HMP. And additional 1% DMSO was used as delivering agent for daidzein and in the corresponding negative controls. The reactions were carried out at ambient temperature. They were continuously monitored by UV spectrometry (at λ = 340 nm). Values are means and range of two determinations.

aromatic ring, whereas the methylpyrene derivatives involve four condensed benzene rings.

Kinetic analyses with the methylpyrene derivatives were complicated by their poor solubility in water, requiring the use of organic delivering solvents and solubilizing regimens (which in general negatively affect kinetic parameters apart from the better solubility). Nevertheless, we could clearly show that HMPs and FPs are much better substrates for ADH2 than the standard substrates ethanol and acetaldehyde. 2-HMP and 2-FP were even better substrates than their positional isomers, possibly because their functional group is located in the most peripheral position of the pyrene nucleus and thus may best be accessible for the enzyme.

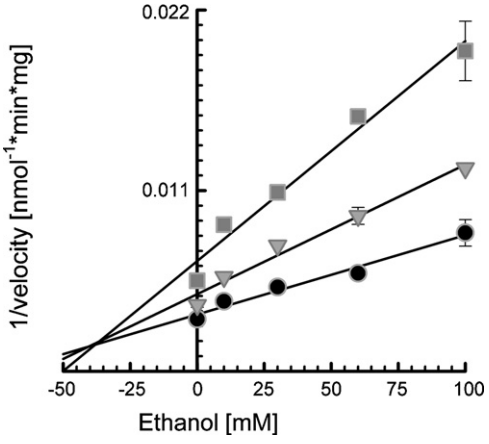

Fig. 6 – Dixon plot of the ADH2-catalyzed oxidation of 1-HMP in the presence of varying concentrations of ethanol. The substrate, 1 HMP, was used at the following concentrations: 60 μM (●), 40 μM (▽) and 20 μM (■). Solubilizing regimen 1 (6% DMSO) was used. The reactions were carried out at 37 °C for 5 min. Afterwards the amount of 1-FP formed was determined by HPLC with fluorescence detection. Values are means and range of two determinations.

We identified and characterized four inhibitors of the ADH2-mediated oxidation of HMPs: ethanol, which is a competing substrate, and three compounds for which an inhibition of ADH2 with other substrates such as ethanol was known from earlier studies. The apparent K_i value of ethanol was 38 mM (0.175%, w/v), a concentration that can be attained in humans by alcohol consumption. 4-Methylpyrazole, a competitive ADH inhibitor clinically used for the treatment of ethylene glycol [32,33] and methanol poisoning [34], showed a somewhat higher apparent K_i value when HMPs rather than ethanol were used as substrates. The reasons for this difference have not been elucidated. They may be technical as solubilizing agents had to be used for HMPs, but not for ethanol. From previous studies it was known that the H_2 receptor antagonist cimetidine [30] and the isoflavone daidzein [29] competitively inhibit ADH2 activity towards ethanol. We confirmed these findings and extended them to a further substrate, 1-HMP. This congruence is not fully trivial, as cimetidine and daidzein differentially affected another ADH form, ADH1C, depending on the substrate used—they

inhibited the oxidation of ethanol, but stimulated the oxidation of 4-HMP (Kollock and Glatt, manuscript in preparation).

The practical significance of such interactions remains to be clarified. There is good epidemiological evidence that consumption of alcoholic beverages increases the incidence of various cancers in humans; by contrast, ethanol did not induce tumours in animals in general when tested alone [35,36]. However, it enhanced the tumorigenicity of certain carcinogens [35]. Likewise, a strong synergism has been observed between alcohol and tobacco smoking for certain malignant tumours in humans, *e.g.* those of the oesophagus [37]. Alk-PAHs are present at high levels in cigarette smoke. For example, 1-methylpyrene has been found in cigarette smoke at a 3.3-fold higher level than that of benzo[*a*]pyrene [38]. And the total of three methylpyrenes exceeds the level of benzo[*a*]pyrene by a factor of 10; in addition dimethylated congeners are present (Seidel, Frank and Glatt, manuscript in preparation). It is therefore possible that ethanol is an indirect carcinogen in humans acting via a reduced ADH-mediated detoxification (which does not exclude additional modes of action). In this context, it would be interesting to see whether other long-term modulations of ADH2 activity—*e.g.* resulting from genetic polymorphism [20] or from dietary and pharmaceutical factors (such as daidzein and cimetidine, respectively) would increase cancer risks in certain situations (*e.g.* involving high exposure to alk-PAHs).

Acknowledgements

Research described in this article was supported by Philip Morris USA Inc. and by Philip Morris International. We thank Dr. Harschadrai Rawel for his assistance on the purification of ADH2 and Martina Scholtyssek for her skilful technical assistance.

REFERENCES

[1] Luch A. The Carcinogenic Effects of Polycyclic Aromatic Hydrocarbons. London: Imperial College Press; 2005.
[2] Thakker DR, Yagi H, Levin W, Wood AW, Conney AH, Jerina DM. Polycyclic aromatic hydrocarbons: metabolic activation to ultimate carcinogens. In: Anders MW, editor. Bioactivation of Foreign Compounds. Academic Press Inc.; 1985. p. 177–242.
[3] Watabe T, Ishizuka T, Isobe M, Ozawa N. A 7-hydroxymethyl sulfate ester as an active metabolite of 7,12-dimethylbenz[*a*]anthracene. Science 1982;215:403–5.
[4] Surh Y-J, Miller JA. Roles of electrophilic sulfuric acid ester metabolites in mutagenesis and carcinogenesis by some polynuclear aromatic hydrocarbons. Chem-Biol Interact 1994;92:351–62.
[5] Glatt HR, Meinl W, Kuhlow A, Ma L. Metabolic formation, distribution and toxicological effects of reactive sulphuric acid esters. Nova Acta Leopoldina NF87 2003;329:151–61.
[6] Rice JE, Rivenson A, Braley J, LaVoie EJ. Methylated derivatives of pyrene and fluorene: evaluation of genotoxicity in the hepatocyte/DNA repair test and tumorigenic activity in newborn mice. J Toxicol Environ Health 1987;21:525–32.
[7] Engst W, Landsiedel R, Hermersdörfer H, Doehmer J, Glatt HR. Benzylic hydroxylation of 1-methylpyrene and 1-ethylpyrene by human and rat cytochromes P450 individually expressed in V79 Chinese hamster cells. Carcinogenesis 1999;20:1777–85.
[8] Glatt HR, Seidel A, Harvey RG, Coughtrie MWH. Activation of benzylic alcohols to mutagens by human hepatic sulphotransferases. Mutagenesis 1994;9:553–7.
[9] Glatt HR, Pauly K, Frank H, Seidel A, Oesch F, Harvey RG, et al. Substance-dependent sex differences in the activation of benzylic alcohols to mutagens by hepatic sulfotransferases of the rat. Carcinogenesis 1994;15:2605–11.
[10] Glatt HR. Sulfotransferases in the bioactivation of xenobiotics. Chem-Biol Interact 2000;129:141–70.
[11] Glatt HR, Pabel U, Muckel E, Meinl W. Activation of polycyclic aromatic compounds by cDNA-expressed phase I and phase II enzymes. Polycyclic Aromat Compd 2002;22:955–67.
[12] Ma L, Kuhlow A, Glatt HR. Ethanol enhances the activation of 1-hydroxymethylpyrene to DNA adduct-forming species in the rat. Polycyclic Aromat Compd 2002;22:933–46.
[13] Theorell H, Yonetani T, Sjöberg B. On the effects of some heterocyclic compounds on the enzymic activity of liver alcohol dehydrogenase. Acta Chem Scand 1969;23:255–60.
[14] Li TK, Theorell H. Human liver alcohol dehydrogenase: inhibition by pyrazole and pyrazole analogs. Acta Chem Scand 1969;23:892–902.
[15] Duester G, Farrés J, Felder MR, Holmes RS, Höög J-O, Parés X, et al. Recommended nomenclature for the vertebrate alcohol dehydrogenase gene family. Biochem Pharmacol 1999;58:389–95.
[16] Vollmann H, Becker H, Corell M, Streeck H. Beiträge zur Kenntnis des Pyrens und seiner Derivate. Justus Liebigs Ann Chem 1937;531:1–159.
[17] Nakasuji K, Akiyama S, Nakagawa M. Linear conjugated systems bearing aromatic terminal groups. VII. Syntheses and electronic spectra of 1,1′- and 2,2′-dipyrenylpoly-ynes. Bull Chem Soc Jpn 1972;45:875–82.
[18] Gerasimenko YE, Shevcbuk IN. Pyrene chemistry. VIII. 4-Acylpyrenes and 3*H*-benz[c,d]pyrene-3-one. J Org Chem (USSR) 1968;4:2120–3.
[19] Foroozesh M, Primrose G, Guo Z, Bell LC, Alworth WL, Guengerich FP. Aryl acetylenes as mechanism-based inhibitors of cytochrome P450-dependent monooxygenase enzymes. Chem Res Toxicol 1997;10:91–102.
[20] Strömberg P, Svensson S, Hedberg JJ, Nordling E, Höög J-O. Identification and characterisation of two allelic forms of human alcohol dehydrogenase 2. Cell Mol Life Sci 2002;59:552–9.
[21] Bullas LR, Ryu J-I. *Salmonella typhimurium* LT2 strains which are r^- m^+ for all three chromosomally located systems of DNA restriction and modification. J Bacteriol 1983;156:471–4.
[22] Maron DM, Ames BN. Revised methods for the *Salmonella* mutagenicity test. Mutat Res 1983;113:173–215.
[23] Glatt HR, Meinl W. Sulfotransferases and acetyltransferases in mutagenicity testing: technical aspects. Meth Enzymol 2005;400:230–49.
[24] Meinl W, Meerman JHN, Glatt HR. Differential activation of promutagens by alloenzymes of human sulfotransferase 1A2 expressed in *Salmonella typhimurium*. Pharmacogenetics 2002;12:677–89.
[25] Laemmli UK. Cleavage of structural proteins during the assembly of the head of bacteriophage T4. Nature 1970;227:680–5.
[26] Dixon M. The determination of enzyme inhibitor constants. Biochem J 1953;55:170–1.
[27] Sharkawi M. Inhibition of alcohol dehydrogenase by dimethyl formamide and dimethyl sulfoxide. Toxicol Lett 1979;4:493–7.

[28] Cho H, Plapp BV. Specificity of alcohol dehydrogenases for sulfoxides. Biochemistry 1998;37:4482–9.
[29] Keung WM. Biochemical studies of a new class of alcohol dehydrogenase inhibitors from *Radix puerariae*. Alcohol Clin Exp Res 1993;17:1254–60.
[30] Stone CL, Hurley TD, Peggs CF, Kedishvili NY, Davis GJ, Thomasson HR, et al. Cimetidine inhibition of human gastric and liver alcohol dehydrogenase isoenzymes: identification of inhibitor complexes by kinetics and molecular modeling. Biochemistry 1995;34:4008–14.
[31] Ditlow CC, Holmquist B, Morelock MM, Vallee BL. Physical and enzymatic properties of a class II alcohol dehydrogenase isozyme of human liver: π-ADH. Biochemistry 1984;23:6363–8.
[32] Brent J, McMartin K, Phillips S, Burkhart KK, Donovan JW, Wells M, et al. Fomepizole for the treatment of ethylene glycol poisoning. N Engl J Med 1999;340:832–8.
[33] Borron SW, Mégarbane B, Baud FJ. Fomepizole in treatment of uncomplicated ethylene glycol poisoning. Lancet 1999;354:831.
[34] Brent J, McMartin K, Phillips S, Aaron C, Kulig K. Fomepizole for the treatment of methanol poisoning. N Engl J Med 2001;344:424–9.
[35] IARC. IARC Monographs on the Evaluation of Carcinogenic Risks, vol. 44. Lyon (France): International Agency for Research on Cancer; 1988.
[36] World Cancer Research Fund. Food, Nutrition and the Prevention of Cancer: A Global Perspective. Washington: World Cancer Research Fund; 1997.
[37] Tuyns AJ. Oesophageal cancer in non-smoking drinkers and in non-drinking smokers. Int J Cancer 1983;32:443–4.
[38] Grimmer G. Prozesse, bei denen PAH entstehen. In: Umweltbundesamt, editor. Luftqualitätskriterien für ausgewählte polyzyklische aromatische Kohlenwasserstoffe. Berlin: Erich Schmidt-Verlag; 1979. p. 54–76.
[39] Meinl W, Pabel U, Osterloh-Quiroz M, Hengstler JG, Glatt HR. Human sulfotransferases are involved in the activation of aristolochic acids and are expressed in renal target tissue. Int J Cancer 2006;118:1090–7.